Bone metastases from prostate, breast and multiple myeloma: differences in lesion conspicuity at short-tau inversion recovery and diffusion-weighted MRI

T PEARCE, FRCR, S PHILIP, FRCR, J BROWN, FRCR, D M KOH, FRCR and P R BURN, FRCR

Department of Diagnostic Imaging, Musgrove Park Hospital, Taunton, UK

Objectives: The objective of this study was to compare the relative conspicuity of bone metastases on short-tau inversion recovery (STIR) and diffusion-weighted MRI (DWI) whole-body MR sequences for breast, prostate and myeloma malignancies.
Methods: 44 whole-body MRI scans were reviewed retrospectively (coronal T_1 weighted, STIR and DWI with $b=800$). On each scan, up to four of the largest bone lesions were identified on T_1 weighting, and the region of interest signal intensity was measured on STIR and DWI, as well as the background signal intensity. The mean lesion signal to background ratio was calculated for each patient and then for each malignancy group.
Results: In prostate cancer patients, the DWI signal/background ratio was greater than that of STIR in 22 out of 24 patients (mean DWI lesion/background ratio 3.91, mean STIR lesion/background ratio 2.31; $p=0.0001$). In multiple myeloma, the DWI ratio was higher in 6/7 patients (DWI group mean ratio 7.59, STIR group mean ratio 3.7; $p=0.0366$). In 13 breast cancer patients, mean STIR and DWI signal/background were similar (DWI group mean ratio 4.13, group mean STIR ratio 4.26; $p=0.8587$).
Conclusion: Bone lesion conspicuity measured by lesion/background signal intensity was higher on DWI $b=800$ than on STIR in patients with prostate cancer and multiple myeloma. DWI should be used in whole-body MR oncology protocols in these conditions to maximise lesion detection.

Metastatic disease to bones can be the only site of distant spread in patients with prostate or breast cancer. Accurate detection of such disease dissemination can be challenging as small-volume disease confined to the marrow cavity may be missed on radionuclear bone scintigraphy or CT imaging. Whole-body (WB) MRI is increasingly used in oncological imaging as a tool to improve detection of bone metastases. Several authors report good results compared with other modalites. Baur-Melnyk et al [1] found WB MRI gave superior detection rate and staging for myeloma compared with CT, and Shortt et al [2], evaluating the same malignancy, concluded that WB MRI performed better than positron emission tomography CT. In prostate and breast patients, Gutzeit et al [3] found WB MRI to rank equally with skeletal scintigraphy for detection of bone lesions, and in some cases detected markedly more metastases. In a recent pooled meta-analysis of published studies, WB MRI showed a pooled sensitivity of 90.0% and pooled specificity of 91.8% for the detection of bone metastases [4].

WB MRI imaging protocols have evolved with time as MRI scanners are now more technologically advanced. Conventional WB MRI studies have typically employed T_1 weighted (T_1W) and short-tau inversion recovery (STIR) sequences [1, 5, 6]. However, more recently, diffusion-weighted sequences are increasingly being utilised [3, 7]. The image contrast from diffusion-weighted MRI (DWI) is based on difference in the mobility of water protons between tissues. As the mobility of water protons is impeded more in tumour than in normal tissues, this results in higher signal intensity returned from tumour tissues on DWI. Nakanishi et al [8] found that adding DWI to T_1 and STIR sequences improved the sensitivity and positive predictive value for detecting bone metastases in a variety of tumour types.

Although WB MRI using combinations of T_1W, STIR and DWI sequences is being applied in clinical practice, it is unclear to what degree DWI improves lesion detection compared with the more widely applied STIR imaging. Clearly, a high lesion-to-background contrast ratio would improve lesion conspicuity and detectability. Hence, the purpose of this study was to determine the relative conspicuity of bone lesions with STIR and DWI sequences for breast, prostate and myeloma malignancies.

Methods and materials

Study population

Consecutive WB MRI examinations from 2009–10 were reviewed retrospectively. The inclusion criteria were: (1) patients with pathologically confirmed prostate, breast or myeloma malignancies; (2) patients who were treatment naïve or showed recent disease progression prompting disease restaging; and (3) patients who had at

Address correspondence to: Dr Paul Burn, Department of Diagnostic Imaging, Musgrove Park Hospital, Taunton TA1 5DA, UK. E-mail: paulburn@gmail.com

least one site of bone disease demonstrated on imaging, which could be corroborated with other imaging findings or followed up by serial MRI examination.

MRI technique

WB MRI examinations were carried out using a 1.5 T MRI scanner (Avanto; Siemens, Erlangen, Germany). In addition to the head and neck receiver coil, surface phase-array receiver coils were deployed across the chest, abdomen and pelvis, together with the peripheral angiographic coil to the upper thigh. The following sequences were acquired from skull vertex to knees in the coronal plane. T_1W: slice thickness 5 mm, repetition time (TR)=644 ms, echo time (TE)=11 ms, field of view (FOV)=500×425 mm, matrix 320×240, parallel imaging factor 2, number of averages 2. STIR: slice thickness 6 mm, TR=5270 ms, TE=112 ms, inversion time=160 ms, FOV 500×425 mm, matrix 320×240, parallel imaging factor 2, number of averages 1. DWI: slice thickness 6 mm, b=800, three scan trace technique, TR=9400 ms, TE=84 ms, FOV 480×330, matrix 192×154, parallel imaging factor 2, number of averages 6, receiver bandwidth 1736 Hz pixel^{-1}.

Image analysis

T_1W images were used to select up to four of the largest bone lesions that appeared as low signal intensity lesions for each patient. Where possible, each target lesion was chosen at different imaging stations in the body. For each lesion, a region of interest (ROI) circle was drawn within each selected lesion on both the STIR and DWI images and the mean signal intensity recorded. The signal intensity of background bone was similarly measured, by placing an ROI on the nearest normal-appearing bone to each lesion, for each of the two sequences.

For each patient, the mean lesion-to-background ratio of all measured lesions was calculated for both STIR and DWI, as a measure of lesion conspicuity. The mean lesion-to-background ratios for all patients of each specific malignancy group were then combined to obtain a group mean lesion-to-background ratio. As the signal intensity ratios were found to be normally distributed (D'Agostino test), the group mean lesion-to-background ratio for STIR and DWI were compared statistically, using the paired Student's t-test. A p-value of <0.05 was taken to be statistically significant.

Results

154 lesions were measured in 44 patients. The following malignancies were represented: prostate 24 patients (79

lesions), breast 13 patients (50 lesions), myeloma 7 patients (25 lesions). Mean ages: prostate 72 years (range 63–86 years), breast 60 years (range 35–86 years) and myeloma 58 years (range 41–69 years).

The mean lesion-to-background ratios for each malignancy for both DWI and STIR are shown in Table 1 and the differences compared statistically. For the prostate cancer group, the mean lesion conspicuity was significantly higher for DWI than for STIR imaging (p=0.0001) and this relationship held true in 21/24 (88%) individual patients (Figure 1a). For the myeloma group, mean lesion conspicuity was also significantly higher for DWI (p=0.0366), being observed in 6/7 (86%) individual patients (Figure 1b). However, among patients with breast cancer, the mean lesion conspicuity for DWI was similar to that of STIR (overall STIR conspicuity was slightly higher, but not statistically significant; p=0.8587); on an individual patient basis, DWI conspicuity was higher than STIR in 9/13 patients (69%; Figure 1c).

Discusssion

Our results show that for the prostate and myeloma groups, mean lesion conspicuity is superior to DWI compared with STIR and that this relationship holds true in most individual patients (Figures 2 and 3). Our results are concordant with those of Luboldt et al [9], who found in a study of 11 patients with prostate cancer that DWI signal-to-noise ratio was higher than that for STIR (p=0.007) [9]. Sommer et al [10] evaluated signal intensities in 81 myeloma patients, and found that DWI signal was higher than STIR in patients with high concentrations of M component (20 g dl^{-1}), although the relationship was reversed in those patients with low concentrations of M components (<20 g dl^{-1}). These results suggest that whole-body DWI technique is potentially more sensitive than conventional STIR imaging for the detection of bone disease in patients with prostate malignancy or multiple myeloma.

However, in the breast cancer group, the picture is more complex. On an individual basis, the majority of breast patients have higher DWI conspicuity, in accordance with the other two malignancies, albeit in a lower percentage of patients (69 vs 88 and 86%). Of note, one breast patient had markedly higher STIR conspicuity than DWI (Figure 4). As a group, the mean lesion conspicuity for breast cancer is similar for the two sequences (indeed slightly higher with STIR). The reason for the apparent difference in group mean conspicuity of DWI relative to STIR for breast compared with the other two malignancies is unknown, but may be related to different cellular microstructure and/or response to treatment.

Table 1 demonstrates the comparative DWI conspicuity of the different malignancy groups (high to low;

Table 1. Lesion-to-background ratios for each malignancy

Malignancy	Mean DWI signal intensity lesion-to-background ratio (range)	Mean STIR signal intensity lesion-to-background ratio (range)	p-value
Prostate	3.91 (1.29–7.25)	2.31 (1.52–3.42)	0.0001
Breast	4.13 (1.99–9.86)	4.26 (2.10–13)	0.8587
Myeloma	7.59 (2.67–14.7)	3.70 (1.15–5.7)	0.0366

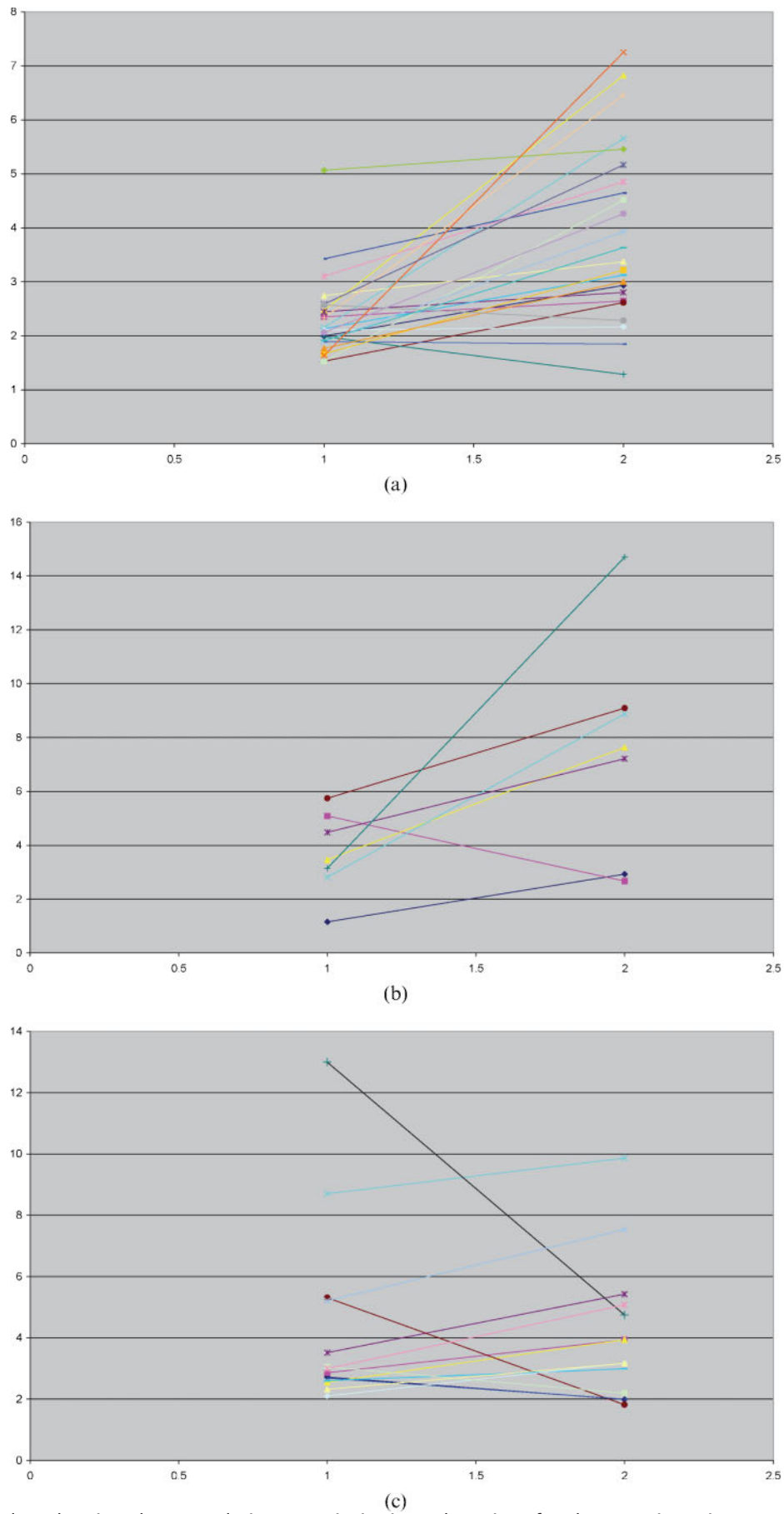DWI, diffusion-weighted MRI; STIR, short-tau inversion recovery.

Figure 1. Ladder plots showing the mean lesion conspicuity in each patient for short-tau inversion recovery (*x*-axis=1) and diffusion-weighted MRI sequences (*x*-axis=2) for each of the three malignancy groups. (a) Prostate cancer, 24 patients; (b) myeloma, 7 patients; (c) breast cancer, 13 patients.

myeloma, breast, prostate). This order could be compared with the degree of sclerosis typically encountered in these lesions (*e.g.* myeloma, lytic; breast, mixed sclerotic/lytic; prostate, sclerotic). However, factors influencing DWI are complex, determined by tumour cellularity and structural organisation [11], which may be further modified by the effects of treatment [12]. Furthermore it could be argued that differences in lesion conspicuity (ratio of lesion-to-background signal intensity) between the three malignancy groups could in part reflect differences in the signal intensity of the background bone marrow, for example due to red marrow persistence in younger patients, or marrow depletion as a consequence of treatment. It would have been possible to control for these variables by also recording the signal intensity of a structure that is relatively invariate (*e.g.* spinal cord or muscle); however, as we wished to focus on the clinical challenge of lesion detection and not the biological behaviour of different tumours, we considered the lesion-to-background bone marrow ratio measurements to be sufficient.

For the DWI sequence, we chose a *b*-value of 800, in line with others [7, 10], as a compromise between obtaining lesion signal (lower values with T_2 shine-through effects) [9] and greater diffusion weighting (higher values). Other researchers have used lower *b*-values: Luboldt et al, $b=200$ [9]; Nakanishi et al, $b=600$ [8]. As we were using the sequence for lesion detection and not primarily for characterisation, we did not use more than one *b*-value and so did not evaluate apparent diffusion coefficient
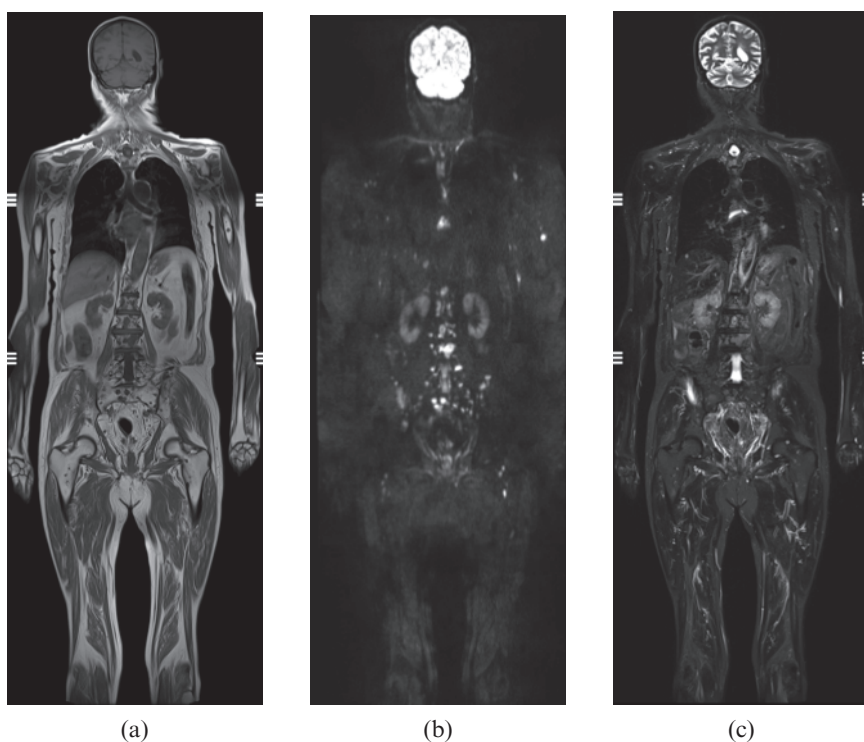

(a)   (b)   (c)

Figure 2. Prostate cancer. Scattered bone metastases, particularly in lumbar spine and pelvis. The lesions are more conspicuous on diffusion-weighted MRI (mean lesion-to-background ratio 4.6) than short-tau inversion recovery (mean lesion-to-background ratio 3.4). Whole-body coronal stitched images. (a) T_1 weighting; (b) diffusion-weighted MRI; (c) short-tau inversion recovery.
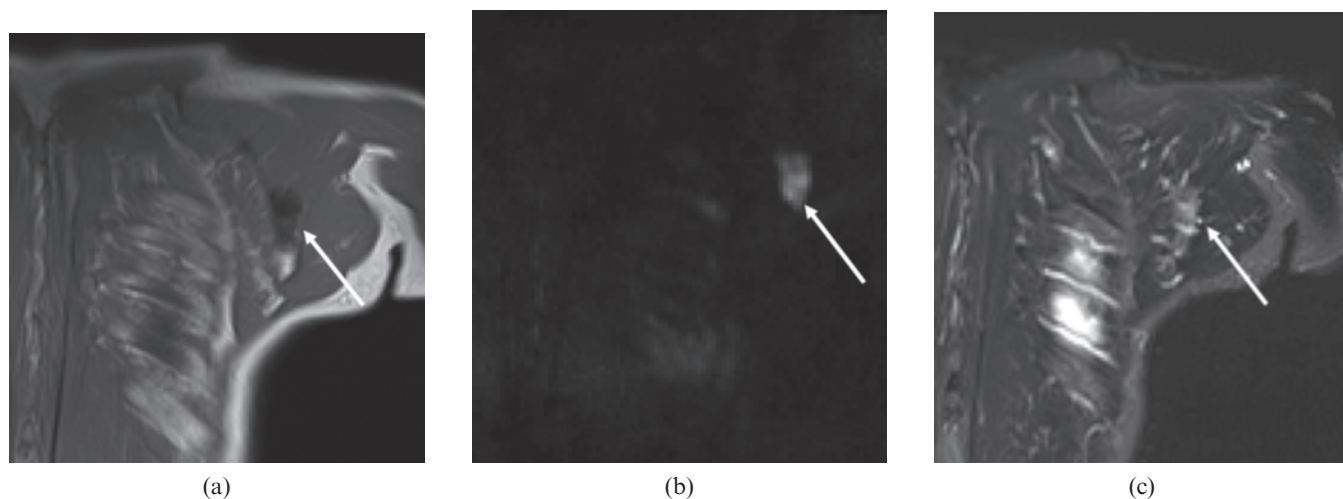

(a)   (b)   (c)

Figure 3. Prostate cancer patient with solitary left scapula metastasis (arrow). The lesion is more conspicuous on diffusion-weighted MRI (lesion-to-background ratio 3.6) than on short-tau inversion recovery (lesion-to-background ratio 1.9). (a) T_1 weighting; (b) diffusion-weighted MRI; (c) short-tau inversion recovery.
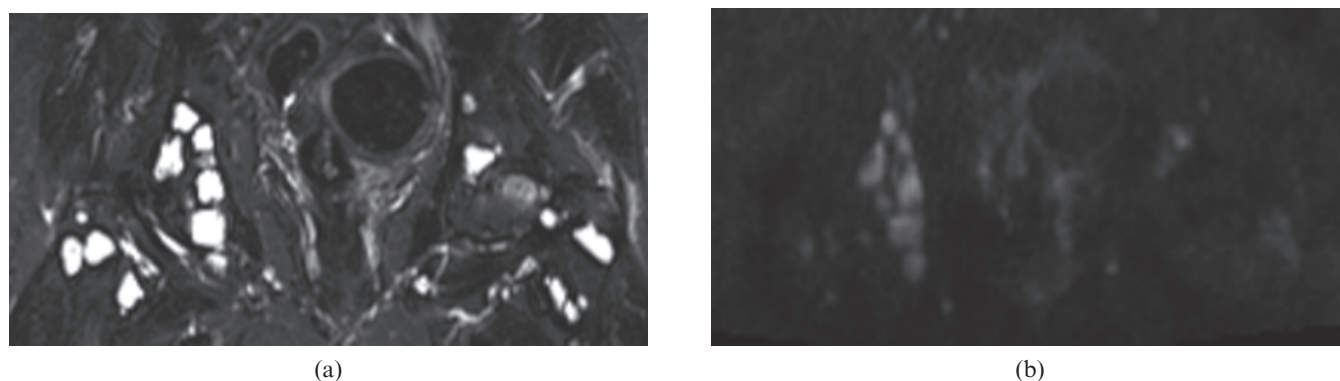
(a)

(b)

Figure 4. Breast cancer patient with multiple lesions in the bony pelvis; in contrast to the relationship in most patients, mean lesion-to-background ratio is higher on short-tau inversion recovery (13) than on diffusion-weighted MRI (4.8). (a) Short-tau inversion recovery; (b) diffusion-weighted MRI.

maps. Clearly the choice of parameters used for both STIR and DWI sequences, particularly the *b*-value, may modify the relative lesion conspicuity between the two sequences. Although STIR lesion conspicuity was inferior in most patients, in a minority of cases the sequence provided superior lesion conspicuity; other advantages of STIR include superior anatomical information and reduced susceptibility to artefacts.

Limitations of our study include the small sample size, and not measuring interobserver and intraobserver variation. In particular, it was sometimes difficult on DWI sequences to accurately place the ROI for background normal bone, as this could be difficult to distinguish from neighbouring tissues. Finally, our patients were a heterogeneous group, and our current observations would benefit from future prospective study in a more homogeneous study population.

In summary, we found lesion conspicuity to be higher with DWI *b*=800 than with STIR in patients with prostate cancer and malignant myeloma. DWI can thus potentially improve the detection of bone disease in these malignancies compared with the conventional whole-body STIR sequence, and may be recommended for inclusion in a whole-body oncology imaging protocol.

References

1. Baur-Melnyk A, Buhmann S, Becker C, Schoenberg S, Lang N, Bartl R, et al. Whole-body MRI versus whole-body MDCT for staging of multiple myeloma. AJR Am J Roentgenol 2008;190:1097–104.
2. Shortt C, Gleeson T, Breen K, McHugh J, O'Connell M, O'Gorman P, et al. Whole-body MRI versus PET in assessment of multiple myeloma disease activity. AJR Am J Roentgenol 2009;192:980–6.
3. Gutzeit A, Doert A, Froehlich JM, Eckhardt BP, Meili A, Scherr P, et al. Comparison of diffusion-weighted whole body MRI and skeletal scintigraphy for the detection of bone metastases in patients with prostate or breast carcinoma. Skeletal Radiol 2010;39:333–43.
4. Wu LM, Gu HY, Zheng J, Xu X, Lin LH, Deng X, et al. Diagnostic value of whole-body magnetic resonance imaging for bone metastases: a systematic review and meta-analysis. J Magn Reson Imaging 2011;34:128–35.
5. Bauerle T, Hillengass J, Fechtner K, Zechmann CM, Grenacher L, Moehler TM, et al. Multiple myeloma and monoclonal gammopathy of undetermined significance: importance of whole-body versus spinal MR imaging. Radiology 2009; 252:477–85.
6. Venkitaraman R, Cook G, Dearnaley DP, Parker CC, Khoo V, Eeles R, et al. Whole-body magnetic resonance imaging in the detection of skeletal metastases in patients with prostate cancer. J Med Imaging Radiat Oncol 2009; 53:241–7.
7. Heusner TA, Kuemmel S, Koeninger A, Hamami ME, Hahn S, Quinsten A, et al. Diagnostic value of diffusion-weighted magnetic resonance imaging (DWI) compared to FDG PET/CT for whole-body breast cancer staging. Eur J Nucl Med Mol Imaging 2010;37:1077–86.
8. Nakanishi K, Kobayashi M, Nakaguchi K, Kyakuno M, Hashimoto N, Onishi H, et al. Whole-body MRI for detecting metastatic bone tumor: diagnostic value of diffusion-weighted images. Magn Reson Med Sci 2007;6:147–55.
9. Luboldt W, Küfer R, Blumstein N, Toussaint T, Kluge A, Seemann M, et al. Prostate carcinoma: diffusion weighted imaging as potential alternative to conventional MR and 11C-choline. Radiology 2008;249:1017–25.
10. Sommer G, Klarhöfer M, Lenz C, Scheffler K, Bongartz G, Winter L. Signal characteristics of focal bone marrow lesions in patients with multiple myeloma using whole body T_1w-TSE, T_2w-STIR and diffusion-weighted imaging with background suppression. Eur Radiol 2011;21:857–62.
11. Rumboldt Z, Camacho D, Lake D, Welsh C, Castillo M. Apparent diffusion coefficients for differentiation of cerebellar tumors in children. AJNR Am J Neuroradiol 2006;27:1362–9.
12. Reischauer C, Froehlich JM, Koh DM, Graf N, John H, Binkert CA, et al. Bone metastases from prostate cancer: assessing treatment response by using diffusion-weighted imaging and functional diffusion maps—initial observations. Radiology 2010;257:523–31.